Methane Hydrate Equilibria in Silica Gels with Broad Pore-Size Distributions

Duane H. Smith
U.S. Dept. of Energy, National Energy Technology Laboratory, Morgantown, WV 26507
and
Dept. of Physics, West Virginia University, Morgantown, WV 26506

Joseph W. Wilder
U.S. Dept of Energy, National Energy Technology Laboratory, Morgantown, WV 26507

Kal Seshadri
Parsons Infrastructure and Technology Group, Morgantown, WV 26505

Equilibrium pressures for the dissociation of methane hydrates confined in silica gel pores of nominal radii 7.5, 5.0 and 3.0 nm were measured over a wide temperature range, and were observed to be higher than those for bulk methane hydrate. A model is presented that allows the pore radius involved in each equilibrium to be determined from these data, so that the model exactly reproduces the experimental equilibrium pressure. Based on this model, pore volume distributions were reconstructed and found to be in good agreement with those obtained from nitrogen desorption isotherms, indicating that hydrate formed nearly uniformly in the available pores.

Introduction

Gas hydrates can be formed from light hydrocarbons such as methane and water at high pressures and ordinary temperatures (or at moderate pressures and low temperatures). The resulting structures are crystalline icelike clathrates where each water molecule is hydrogen bonded to its nearest neighbors, forming a cagelike structure in which the gas molecules are occluded. The discovery of natural gas hydrate deposits in arctic regions and in subseafloor deposits in outer continental shelves has stimulated interest in the study of gas hydrate formation/decomposition in porous media. It is estimated that the volume of natural gas in these deposits is enormous, representing large potential sources of a clean fuel. The eventual production of natural gas from these reservoirs is of great interest to both the private and public sectors.

The study of the synthesis and decomposition of gas hydrates in porous media is important to gaining an understanding of the conditions at which gas hydrates form or dissociate in gas reservoirs. Several such studies have been reported in the literature. Studies by Makogon (1981) in sandstones with nominal pore radii of 5.7, 5.0, and 3.5 μm suggested that the pressure required for hydrate formation increased as the pore size was decreased. Since the equilibrium pressure for the dissociation of hydrates and the thermodynamic properties in large pores are apparently nearly identical to those in the bulk (Kamath, 1984), one needs to conduct experiments in much smaller pores to quantify pore-size effects. Differences in chemical potentials and interfacial forces between the bulk and pore water affect hydrate formation in such pores. In addition, many porous materials have broad pore-size distributions that also affect the formation and dissociation characteristics of the hydrate. Therefore, the study of hydrate formation/dissociation is much more complex for porous media than for the bulk. Handa and Stupin (1992) studied methane and propane hydrates in silica gel of 7.5-nm nominal pore radius, and Uchida et al. (1990) investigated the properties of methane hydrate in three porous Vycor glass

Correspondence concerning this article should be addressed to D. H. Smith.
Current address of J. W. Wilder: Dept. of Mathematics, PO Box 6310, West Virginia University, Morgantown, WV 26506.

samples with pore radii of 25 nm, 15 nm, and 5 nm. In a recent work (Seshadri et al., 2001) the authors presented measurements for propane hydrate formation in silica gels of nominal pore radii of 7.5 nm, 5.0 nm, 3.0 nm, and 2.0 nm. The work just mentioned (Handa and Stupin, 1992; Seshadri et al., 2001) provided information on the effect of pore size on the formation of this Structure II hydrate.

Henry et al. (1999) and Clarke et al. (1999) have proposed interpretations of the data of Handa and Stupin (1992) based on the addition of a capillary pressure term to the statistical-thermodynamic model of van der Waals and Platteeuw (1959). However, these interpretations did not adequately reproduce the experimental equilibrium pressures of Handa and Stupin (1992). As suggested by the authors of these interpretations (Henry et al., 1999; Clarke et al., 1999), the discrepancies may be due to the assumption that a single pore size can adequately represent samples that in reality involve rather broad distributions of pore sizes (Handa et al., 1992). Because hydrates formed in porous media have one additional degree of freedom, the equilibrium curve in *P-T* space of bulk hydrates is replaced by an equilibrium surface in *P-T-r* space, the quadruple point is replaced by a quadruple line, and simple regressions of experimental *P-T* data cannot be used to find the resulting multiple quadruple points.

To solve the problems of assuming a single pore size, we propose a modified model that recognizes the broad distribution of pore sizes present in many porous media. This model, in addition to explaining the source of previous discrepancies, also allows the reconstruction of the pore-volume distribution present in the porous medium. A very different approach involving a completely different method of predicting hydrate equilibria and that imposes an assumed pore-size distribution has been proposed by Klauda and Sandler (2001). More experimental data are needed to further test these models, facilitate future modeling efforts, and gain a better understanding of these complex systems. To meet these needs we have performed experiments and investigated the properties of methane hydrate in the same silica gel samples (nominal pore radii of 3, 5, and 7.5 nm) as those used previously (Seshadri et al., 2001) for propane hydrate. These two sets of data allow a test of the multiple pore-size model for both Structure I (methane) and Structure II (propane) hydrates. Such data for a range of pore sizes, all of which involve capillary effects that strongly affect the equilibrium pressure, should help to further delineate the effects of pore size on key equilibria for important components of natural gas.

Experimental Methods

Methane with minimum purity of 99.97 mol % was obtained from Matheson. Nitrogen desorption and adsorption studies using Quantachrome Corp Autosorb-1 equipment were used to determine the pore-volume distribution (Lowell and Shields, 1991) and total pore volume of each of the silica gel samples used in the experiments. A high-pressure cell (Seshadri et al., 2001) about 30 mL in volume was loaded with around 140 5-mm-diameter glass beads, and a slurry consisting of liquid nitrogen and silica gel containing pore water was poured over the glass beads, coating them with the silica gel. The sealed cell was then connected to a vacuum manifold and cooled in liquid nitrogen. The cell was evacuated to about 50 mtorr, and held at that pressure for 30 min to remove air. The cell was transferred to a temperature-controlled chiller (Neslab Model RTE 140), and then connected to the methane cylinder and the transducer. The bath temperature was read with a Hart Scientific model 1006 MicroTherm thermometer with a sensitivity of 0.001 K. The bath temperature was stable to within $\pm 0.4\%$. The pressure measurements were made with a 20.78-MPa full-scale transducer (Setra 204E transducer and Setra Datum 2000 reader), which was calibrated by the dead-weight method. The accuracy of the transducer was 0.2% of full scale. The experimental methods used to form the hydrate and to measure the equilibrium temperatures and pressures during its subsequent dissociation are the same as those used previously (Handa and Stupin, 1992; Seshadri et al., 2001), and entail a stepwise increase of the temperature and the subsequent reestablishment of equilibrium at each new temperature. In this work we report equilibrium pressure–temperature data for the dissociation of methane hydrates in the same four silica gel samples (nominal pore radii of 2, 3, 5, and 7.5 nm) as those used previously for propane (Seshadri et al., 2001).

Results and Discussion

Silica gel properties

The physical properties of the silica gel used here have been reported previously (Seshadri et al., 2001). The pore-size distributions for these gels were found by applying the method described in Lowell and Shields (1991) to the Autosorb-1 data. The isotherms obtained from the Autosorb-1 are shown in Figure 1. As can be seen in the figure, the isotherms for the silica gels with nominal pore radii of 7.5, 5.0, and 3.0 nm resemble Type A hysteresis, as identified by de Boer (1958). This type of hyteresis is usually associated with cylindrical pores open at both ends (Lowell and Shields, 1991).

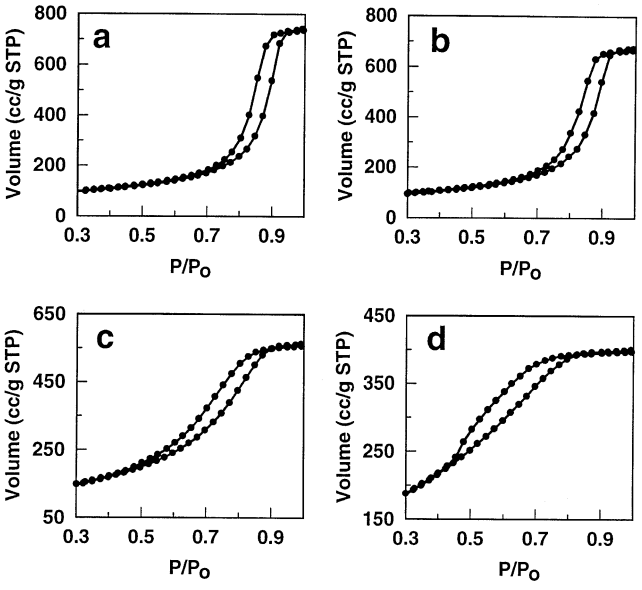

Figure 1. Adsorption/desorption hysteresis for nominal 7.5 (upper-left), 5.0 (upper-right), 3.0 (lower-left), and 2.0 nm (lower-right) silica gel pores based on the Autosorb-1 data.

Table 1. Equilibrium Pressure–Temperature Data for Methane Hydrate in Silica Gel Pores of Various Nominal Radii

7.5 nm		5.0 nm		3.0 nm		2.0 nm	
T (K)	P (MPa)	T (K)	P (MPa)	T (K)	P (MPa)	T (K)	P (MPa)
263.0	2.59	259.0	2.42	253.0	2.08	244	1.60
263.5	2.62	260.0	2.49	254.0	2.13	245	1.66
264.0	2.65	261.0	2.52	255.0	2.19	246	1.72
264.5	2.68	262.0	2.56	257.0	2.27	247	1.75
265.0	2.71	263.0	2.59	258.0	2.34	248	1.81
265.5	2.73	264.0	2.67	259.0	2.42	249	1.84
266.0	2.78	265.0	2.77	260.0	2.48	250	1.89
266.5	2.83	266.0	2.85	261.0	2.56	251	1.95
267.0	2.89	267.0	2.93	262.0	2.66	252	2.00
267.5	2.94	268.0	3.04	263.0	2.79	253	2.05
268.0	3.00	269.0	3.17	264.0	2.91	254	2.08
269.0	3.12	270.0	3.33	265.0	3.03	255	2.15
270.0	3.30	271.0	3.47	266.0	3.18	256	2.18
271.0	3.49	272.0	3.67	267.0	3.35	257	2.23
272.0	3.74	273.0	3.90	268.0	3.53	258	2.29
273.0	3.98	274.0	4.11	269.0	3.72	259	2.34
274.0	4.26	275.0	4.21	270.0	3.85	260	2.40
		276.0	4.22	271.0	4.04	261	2.46
				273.0	4.21	262	2.50
						263	2.54
						264	2.58
						265	2.62
						266	2.66

Methane hydrate properties

The equilibrium pressure–temperature data for the silica gel samples (corrected for the vapor pressure of water) are given in Table 1, and those for the silica gel samples having nominal pore radii of 3, 5, or 7.5 nm are shown graphically in Figure 2 (the 2-nm data have been reserved for a separate discussion). Also included in the figure are measured data for bulk methane hydrate (Sloan, 1997). In Figure 2, some of the data for the silica gels with nominal pore radii of 5.0 or 7.5 nm appear to coincide. The equilibrium pressure at a specific temperature is expected to depend on the pore radius for such sized pores as those considered here (Makogon, 1981; Seshadri et al., 2001). Furthermore, if the data for the nominal 7.5-nm pores presented in Figure 2 are compared with the data in the literature (Handa and Stupin, 1992), there is a small difference that increases as the temperature increases. Both of these apparent discrepancies can be explained by means of a conceptual model for hydrate decomposition in a porous medium involving a broad pore-size distribution.

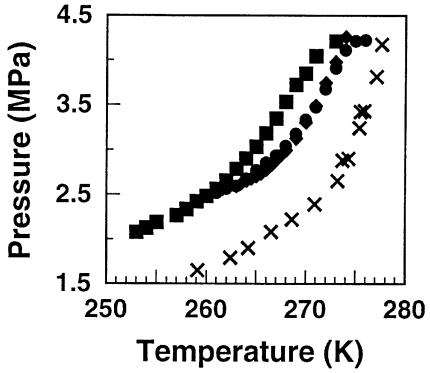

Figure 2. Experimentally measured equilibrium pressures in silica gels of nominal pore radii 3 (■), 5 (●), and 7.5 (♦) nm.

Also shown are results for bulk hydrate formation (×).

If the modifications suggested by Henry et al. (1999) to model hydrate formation in porous media are made to the standard statistical thermodynamic model used for bulk hydrates, the result can be written in the form of Eq. 1

$$\frac{\Delta\mu_W^0}{RT_0} - \int_{T_0}^{T_f}\frac{\Delta H_w}{RT^2}\,dT + \int_0^{P_f}\frac{\Delta V_w}{RT_f}\,dP - \ln(\gamma_w X_w) + \sum_i \eta_i \ln(1-Y_i) + V_L\frac{2\cos(\theta)\sigma_{hw}}{rRT_f} = 0. \quad (1)$$

In this article we propose using Eq. 1 along with equilibrium temperature–pressure data to determine what size pores are involved in the equilibria observed experimentally for hydrates in porous media such as silica gel. In Eq. 1, T_f and P_f are the temperature and pressure at which the hydrate forms, T_0 is the temperature of the standard reference state (T = 273.15 K, $P = 0$), and $\Delta\mu_W^0$ is the chemical potential difference for the reference state. The second term on the left-hand side of Eq. 1 accounts for the temperature dependence of the chemical potential difference (at zero pressure) by assuming $\Delta H_W = \Delta H_W^0 + \int_{T_0}^{T}\Delta C_p(T')\,dT'$, where ΔH_W^0 is a reference enthalpy difference between the empty hydrate lattice and the pure water phase at the reference temperature. The temperature dependence of the heat capacity difference between these two states is modeled as (Holder et al., 1988) $\Delta C_p(T') = \Delta C_p^0 + b(T' - T_0)$, where ΔC_p^0 is the reference heat capacity difference, and b is a constant. The third term on the lefthand side of Eq. 1 corrects for the pressure dependence, and involves ΔV_W, the volume difference between the empty hydrate and the pure solid or liquid water (at T_0), and is assumed constant (but different for solid or liquid water). The fourth term is a correction to the chemical potential of pure water due to the solubility of th guest molecule [which can be neglected for methane (Munck et al., 1988)]. We note that the maximum errors between the experimental data and the model predictions for bulk hydrate formation are 1.3 and 2.6% for methane and propane, respectively, over a temperature range from 260 K to 276 K using the model parameters given in Table 2 and ignoring the gas solubility in water. The fifth term involves η_i, which is the number of cavities of type i in the hydrate lattice. The probability of a cavity of type i being occupied by the guest molecule is denoted by Y_i, and is given in terms of the fugacity of the hydrate guest in the gaseous state (f) and the Langmuir adsorption constant (C_i) by $Y_i = C_i f/(1 + C_i f)$. In the present model, the temperature dependence of the Langmuir constants is accounted for by using the form presented by Munck et al. (1988), $C_i = (A_i/T)\exp(B_i/T)$, where A_i and B_i are experimentally fit parameters, and are dependent on which guest molecule is present. Other researchers have used Kihara potential functions to model these constants. Since this approach also involves parameters that are adjusted to fit the model predictions to experimental data, we use the preceding formulation because of its ease of use. The last term on the lefthand side

Table 2. Parameter Values for Hydrate Formation

Property	Unit	Bulk Value for Methane	Bulk Value for Propane
$\Delta\mu_W^0$	J/mol	1,263*	883.8*
$(\Delta H_W^0)_{ice}$	J/mol	1,389*	1025*
$(\Delta H_W^0)_{liq}$	J/mol	−4,622*	−4,986*
ΔC_p^0	J/mol·K	$-34.583^{\dagger\dagger}T > T_0$	$-38.8607^{\dagger\dagger}T > T_0$
		$3.315^{\dagger\dagger}T < T_0$	$1.029^{\dagger\dagger}T < T_0$
ΔV_w	m^3/mol	2.9959×10^{-6}**	3.39644×10^{-6}**
σ_{hw}	J/m^2	0.0267	0.0267
b	J/mol·K^2	$0.189^{\dagger\dagger}T > T_0$	$0.18090^{\dagger\dagger}T > T_0$
		$0.121^{\dagger\dagger}T < T_0$	$0.00377^{\dagger\dagger}T < T_0$
A_i	K/atm	$0.0007372^{\dagger}$ (small cavity)	$0.0^{\dagger}$ (small cavity)
		$0.025354^{\dagger}$ (large cavity)	$0.0017634^{\dagger}$ (large cavity)
B_i	K	$3{,}267.99^{\dagger}$ (small cavity)	$0.0^{\dagger}$ (small cavity)
		$2{,}782.94^{\dagger}$ (large cavity)	$4{,}945.94^{\dagger}$ (large cavity)

*Parameter values taken from Sloan (1997).
**Add 1.6×10^{-6} m^3/mol in the liquid water region to account for the difference in molar volume between liquid water and ice.
†These values were obtained by fitting the model to the data for bulk methane and propane hydrate formation found in Sloan (1997).
††Parameter values taken from Holder et al. (1988).

of Eq. 1 shows the effect of capillary pressure on the chemical potential difference between the empty hydrate lattice and the pure-water phase. Here, V_L is the molar volume of water in the pure-water state, θ is the wetting angle between the pure-water phase and the hydrate (Henry et al., 1999), σ_{hw} is the surface tension between the water and hydrate phases (Henry et al., 1999), and r is the radius of the pore.

Equation 1 is used to determine a value of r for each experimental temperature and pressure (T_f, P_f). The value of r is found by application of the secant method, augmented by bisection in the event that the former method failed (Cheney and Kincaid, 1994). The Soave–Redlich–Kwong equation of state was used to calculate the fugacity of the gas. The parameter values used in the calculations can be found in Table 2.

Using Eq. 1 along with the data in Figure 2 leads to the calculation of the effective pore radius involved in each equilibrium. These calculations are based on the following conceptual model for hydrate decomposition in a porous medium with a broad pore-size distribution. As a simplistic representation of such a medium, consider a bundle of tubes with a distribution of tube radii $r_1 < r_2 < r_3 < r_4 < r_5 \cdots$. If we had a series of samples, each exclusively made up of one size tube, then the equilibrium pressures necessary to stabilize the hydrate in the various samples would be given by P_1, P_2, P_3, P_4, P_5, $\cdots$, with $P_1 > P_2 > P_3 > P_4 > P_5 \cdots$. A more realistic representation of porous media includes a distribution of these tubes of different radii such that in a given sample there are N_i tubes of radius r_i. Let the total volume of gas present (as hydrate) in tubes of radius r_i be equal to V_i^g. Now consider a sample of porous medium with various size tubes where the tubes are filled with hydrate and the reaction chamber is kept under conditions such that the hydrate is stable for all tube sizes. As the temperature is raised, the point will eventually be reached where the gas pressure in the chamber is not sufficient for all of the hydrate to remain stable, and some of it will start to decompose. Since smaller radii tubes require larger pressures for their hydrate to remain stable, hydrate in the smallest tubes will be the first to decompose. As the hydrate in the smallest tubes decomposes, gas is given off, raising the pressure in the headspace (the free space exterior to the porous medium and interior to the reaction chamber). If the volume V_1^g (the total volume of gas available from tubes of radius r_1) is more than sufficient to raise the pressure up to P_1 (the pressure necessary to stabilize the hydrate in tubes of radius r_1 at the current temperature), then equilibrium will be reestablished before all of the tubes of radius r_1 are exhausted, and the experimentally observed pressure at this temperature will be that which would be observed if the medium were solely made up of tubes having this radius. If, due to the volume of headspace, these tubes do not contain a large enough volume of gas to raise the pressure by the required amount, then all of the hydrate in tubes of this size will decompose, and that in the next size tubes (having radii r_2) will begin to decompose. If the total volume from these two tubes sizes ($V_1^g + V_2^g$) is more than sufficient to raise the pressure up to P_2, then not all of the hydrate in this size tube will decompose, and the experimentally observed pressure at this temperature will be that which would be observed if the medium were solely made up of tubes having radius r_2. Therefore, with this conceptual model for hydrate decomposition in porous media, at each temperature the measured equilibrium pressure corresponds to that for a single-size tube, but the size of the tube will vary as the temperature is varied. In addition, exactly which size tube is involved in the equilibrium at a specific temperature will depend on the relative sizes of the headspace and the amount of gas present in the form of hydrate.

For each point (T_i, P_i) of the pressure equilibrium curves in Figure 2, there is a corresponding r_i that can be found from Eq. 1 that allows the model to exactly reproduce the measured equilibrium pressure. These data can then be used to calculate the volume of the pores from which hydrate decomposed to cause the pressure increase from P_i (at temperature T_i) to pressure P_{i+1} (at temperature T_{i+1}). To determine the distribution, the molar volume of the gas, υ_i is calculated by means of its equation of state for each experimental temperature and pressure (T_i, P_i). The change in the number of mols of gas in the system in going from state i to state $i+1$ is then given by

$$\Delta n_{i,i+1} = V_{sys}\left(\frac{1}{\upsilon_{i+1}} - \frac{1}{\upsilon_i}\right), \tag{2}$$

where V_{sys} is the volume of the headspace. Given that the number of gas molecules contained in a unit cell of hydrate is n_{cell}, and that the volume of each unit cell is V_{cell}, the total volume of the pores from which the hydrate decomposed to cause the pressure increase from P_i to P_{i+1} per gram of silica gel is given by

$$\Delta V_{i,i+1} = \frac{V_{cell}N_A}{n_{cell}w_{gell}}\Delta n_{i,i+1} = \frac{V_{cell}V_{sys}N_A}{n_{cell}w_{gell}}\left(\frac{1}{\upsilon_{i+1}} - \frac{1}{\upsilon_i}\right), \tag{3}$$

where w_{gell} is the weight of the silica gel used in the experiment, and N_A is Avogadro's number. While V_{cell} is known and n_{cell} can be estimated based on the fractional occupancy of the cages, V_{sys} and w_{gell} are not known for some of the results in the literature. In addition, this only gives an estimate of the volume of water involved in the formation of hydrate, and would not include the volume occupied by water not involved in this process (which may be significant for small pores). To compensate for these difficulties, and for comparison purposes, the pore volumes based on the hydrate data and those obtained from the Autosorb-1 data have been normalized by dividing each by the largest pore volume it contained. The results of these calculations are shown in Figures 3a–3c for the silica gels having nominal pore radii of 7.5, 5.0, or 3.0 nm, respectively. It should be noted that the points in these figures should be interpreted as indicating the tops of bars having a height showing the indicated normalized pore volume, and whose width extends from the indicated point to the next largest radius at which there is a data point. This is shown explicitly in Figure 4 for the nominal 7.5-nm case. As can be seen in Figure 4, it is difficult to interpret these results in this form, and becomes impossible if more than two sets of data are compared (as will be done below). As a result, for clarity of presentation we present our results in the form of Figure 3.

Summing the partial volumes depicted in Figure 3 as one progresses to larger r values allows calculation of the cumulative pore volume for pores up to and including any desired radius. Since reconstructing the pore volumes from measured hydrate equilibrium data involves some parameters (such as sample size and headspace volume) that are not always readily available (especially for data found in the literature), and because sometimes there is an unknown amount of water in the pores that is not converted to hydrate, a multiplicative scale factor must be applied to scale the reconstructed cumulative pore volume to the same magnitude as the one obtained from the Autosorb-1 data. This factor was obtained for each data set by examining the last cumulative volume from the reconstruction and scaling it to fall on the corresponding curve (Figure 5) from the Autosorb-1 data. This same scale factor was then used for all of the points on the reconstructed cumulative pore-volume curve. We note that because of the use of these scale factors we can only compare the shape and relative magnitudes in Figures 3 and 5, not their absolute magnitudes. The results of these calculations are shown in Figures 5a–5c for the silica gels that have nominal pore radii of 7.5, 5.0, and 3.0 nm, respectively, based on the data in Figure 2. We note the strikingly good agreement that can be seen in both Figure 3 and Figure 5. As pointed out by a reviewer, the ability of the single scale factor to allow the pore-volume distribution to be reconstructed with the accuracy seen in Figures 3 and 5 may indicate that the per-

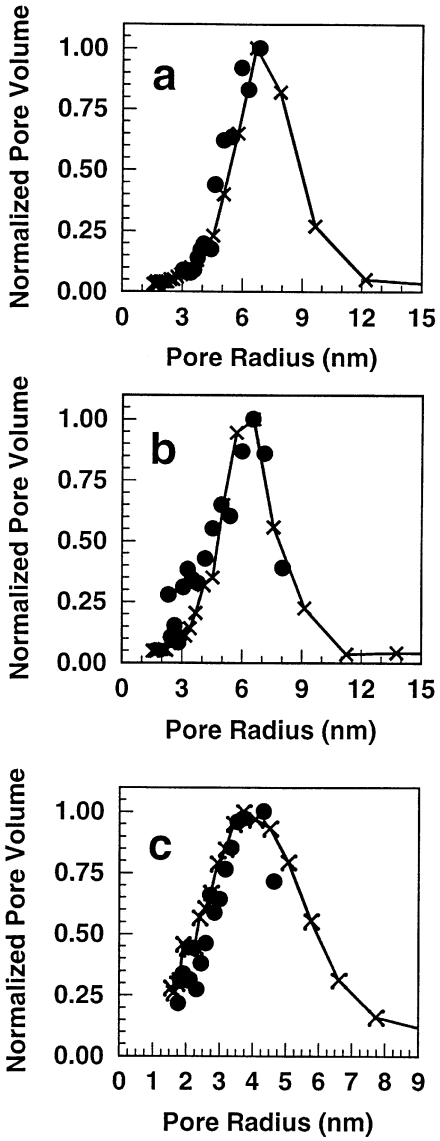

Figure 3. Normailzed pore volume distributions reconstructed from the experimental data in Figure 2 (●) for silica gels with nominal (a) 7.5-nm, (b) 5.0-nm, and (c) 3.0-nm pore radii.

Also shown are the results based on the Autosorb-1 data (solid traces with ×).

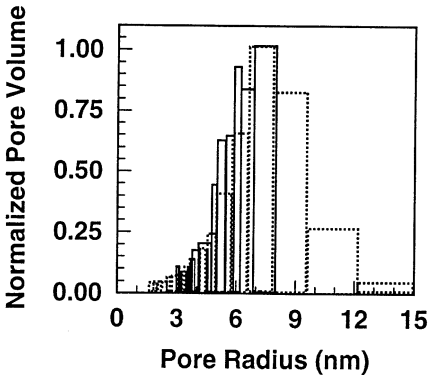

Figure 4. Normalized pore volume distributions reconstructed from the experimental data in Figure 2 (—) for silica gels with nominal 7.5-nm pore radii.

Also shown are the results based on the Autosorb-1 desorption isotherms (· · · · ·).

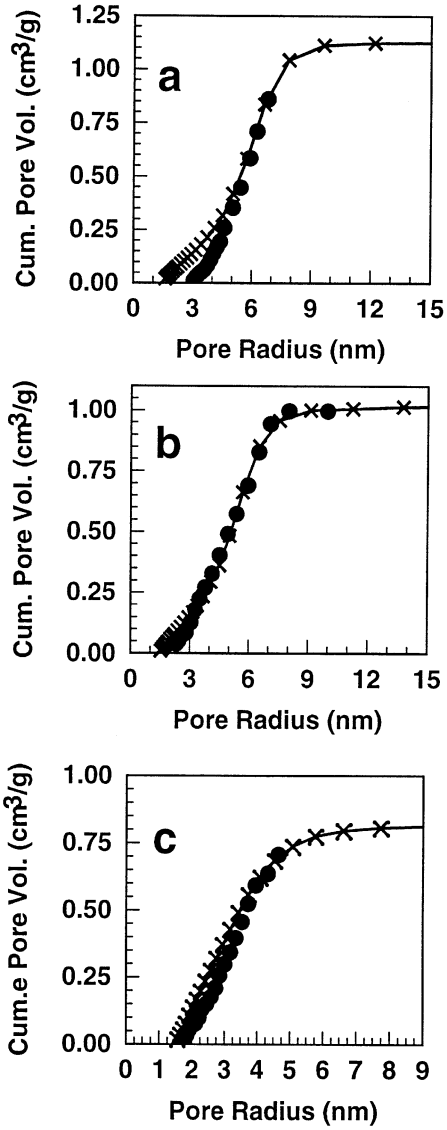

Figure 5. Cumulative pore volumes (●) reconstructed from the experimental data in Figure 2 for silica gels with nominal (a) 7.5-nm, (b) 5.0-nm, and (c) 3.0-nm pore radii.

Also shown are the results based on the desorption isotherms (solid traces with ×).

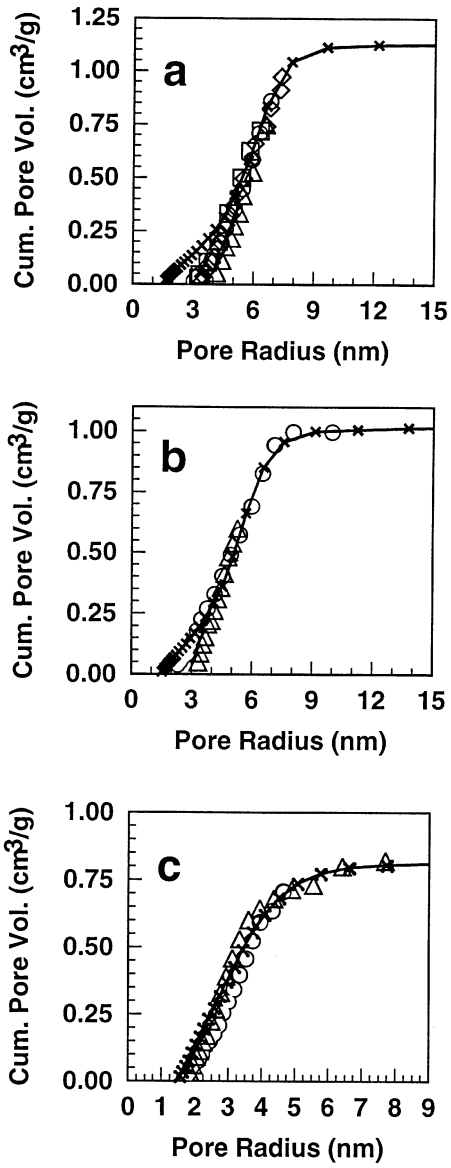

Figure 6. Cumulative pore volumes reconstructed from the experimental data in Figure 2 for methane hydrate (○) and propane hydrate reported in Seshadri et al. (2001) (△) for silica gels with nominal (a) 7.5-nm, (b) 5.0-nm, and (c) 3.0-nm pore radii.

Also shown are the results based on the desorption isotherms (solid traces with ×), and reconstructions based on the data by Handa and Stupin (1992) for methane (□) and propane (◇).

cent conversion of water to hydrate was the same in all of the different size pores involved in the various equilibria used to arrive at a specific reconstruction.

Figure 6 compares reconstructions based on propane hydrate equilibrium pressures reported by the authors elsewhere (Seshadri et al., 2001) for the nominal 7.5-, 5.0-, and 3.0-nm silica gels, and on similar data reported by Handa and Stupin (1992) for the nominal 7.5-nm silica gel with the cumulative pore volumes from the methane hydrate data (Figure 5). As can be seen in Figure 6, there is good agreement between the pore volume reconstructed from experimental data for the Structure I (methane) and Structure II (propane) hydrates. This agreement helps to validate this model for the interpretation of hydrate equilibria in porous media that have broad pore-size distributions.

The reconstructions in Figures 3, 5, and 6 are, as discussed in detail earlier, based on hydrate equilibrium data. Their importance lies not so much in the fact that they represent an indirect method to determine pore-volume distributions, but that they represent a method to get information on what fraction of the total available pore volume at each pore size was filled by hydrate. While standard techniques such as ni-

trogen adsorption can be used to determine the pore-volume distribution for a porous medium, this obviously gives no information concerning where in the medium the hydrate will form. Comparison of the reconstructions discussed earlier with the results of nitrogen adsorption studies indicates that in the experiments reported here for methane, the hydrate formed in most of the available pore space. Small, localized regions in Figure 3 where the reconstructed volumes lie above or below the nitrogen adsorption results are most likely due to scatter in the experimental hydrate equilibrium pressures. Figure 3c shows a consistent trend that the reconstructed volumes for the 3-nm sample lie below those of the nitrogen adsorption results for many pore radii. This indicates pore sizes in this sample where a small portion of the available volume was not filled with hydrate.

Since the equilibrium pressure observed during the dissociation of hydrate in a porous medium depends on the pore radius as well as the temperature, the data depicted in Figure 2 are projections onto the (T, P) plane of a set of points that lie on a surface in (r, T, P) space. In addition to being used to determine the relevant pore sizes involved in each of the equilibria represented by the data in Figure 2, Eq. 1 also can be used to calculate the complete (r, T, P) surface. The results of carrying out these calculations are shown in Figure 7, where the equilibrium envelope for methane hydrate in porous media is shown as a surface. Also shown (dotted trace) is the curve representing the quadruple-point temperature and pressure as a function of r. As can be seen in the figure, the melting point of water (Clennell et al., 1999) and quadruple point of the hydrate depend on pore size, and all of the experimental data are for the equilibrium of hydrate with gaseous methane and liquid water.

Examination of Figures 7 and 8 shows that pore size has a dramatic effect on the equilibrium pressure when the equilibrium involves liquid water. Since the melting temperature of water (and thereby the quadruple point for the hydrate) is affected by pore size (Clennell et al., 1999), the relative

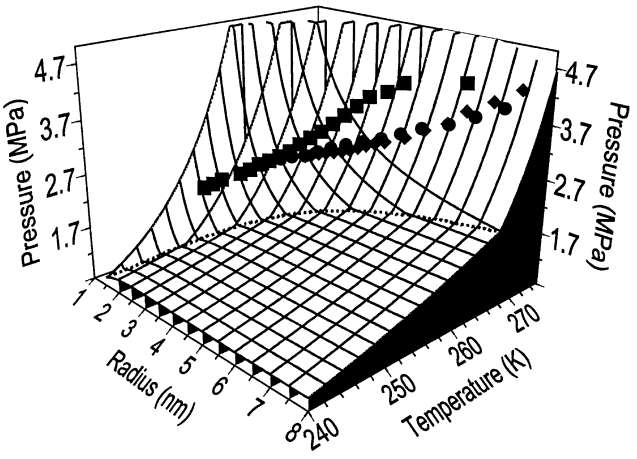

Figure 7. Calculated equilibrium pressure as a function of temperature and pore radius for methane hydrate formation.

The quadruple-point temperature–pressure curve is indicated by the dotted trace. Also shown are the experimentally measured equilibrium pressures in silica gels of nominal pore radii 3 (■), 5 (●), and 7.5 (♦) nm.

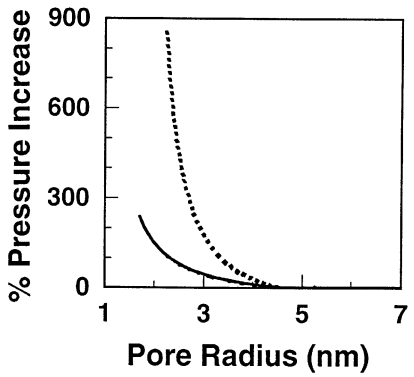

Figure 8. Percent increase in calculated equilibrium pressure above the bulk equilibrium pressure at 263 K for methane (solid trace) and propane (dotted trace) hydrates as functions of pore radius.

change in the equilibrium pressure in a porous medium with respect to that in the bulk can be very large. For example, Figure 8 shows the percent increase in the equilibrium pressure for methane hydrate (solid trace) as a function of pore radius at a temperature of 263 K. The melting point of water in a pore can be calculated from (Clennell et al., 1999):

$$T_m^{\text{pore}} = T_m^{\text{bulk}}\left[1 - \frac{2\sigma_{iw}}{\rho_w \Delta H_{fw} r_b}\right].$$

Here, T_m^{bulk} is the bulk melting temperature (273.15 K), σ_{iw} is the surface tension between water and ice (0.0267 J/m^2) (Clennell et al., 1999), ρ_w is the specific density of water (1,000 kg/m^3), ΔH_{fw} is the specific enthalpy of fusion of bulk water (333 kJ/kg), and r_b is the effective pore radius. At 263 K, water in pores with radii larger than 4.3 nm would be in the form of ice, while that in pores smaller than this would be liquid. As can be seen in Figure 8, at 263 K hydrate in pores with radii larger than 4.3 nm has the same equilibrium pressure as bulk hydrate. This results from the assumption of the model of zero surface tension between hydrate and water ice. Below this point, however, the water is in a liquid form and the surface tension between the liquid water and the hydrate affects the equilibrium pressure, as indicated by Eq. 1. Note that as the pore radius decreases, the percent increase in the equilibrium pressure approaches 250%. Also shown in the figure are the results of a similar calculation for propane hydrate. As can be seen, this Structure II hydrate former results in an increase of over 900% for small radii. We note that the Structure II hydrate former (propane) has an equilibrium pressure that is about 1/20th of the equilibrium pressure of the Structure I hydrate former (methane) at this temperature. Since many Structure II hydrate formers have equilibrium pressures that lie below Structure I hydrate formers, the relative importance of the last term in Eq. 1, which is due to capillary effects, may be larger for Structure II hydrate formers. Testing of this generalization would necessitate the consideration of other Structure I and Structure II formers that both follow the pattern for relative equilibrium pressures just noted (such as ethane and carbon dioxide), and those that do not (such as hydrogen sulfide).

Summary

Handa and Stupin (1992) previously studied the formation of propane and methane hydrates in silica gel with nominal pore radius of 7.5 nm. Adequate study of the effects of capillary pressure on hydrate formation in small pores requires a series of experiments on samples with various nominal pore sizes. The failure of models presented in the literature (Clarke et al., 1999; Henry et al., 1999) to accurately predict the observed equilibrium pressures (Handa and Stupin, 1992) implies that data for a range of pore sizes may be necessary for model-validation studies. The recent work of Uchida et al. (1999) on methane hydrate formation in Vycor glass with nominal pore radii of 10, 30, and 50 nm considered such a series; however, the results for the nominal 30- and 50-nm pores were very close to those for the bulk. In this work, we have considered a series of pore sizes, all of which clearly show capillary effects. In addition, both conceptual and mathematical models have been used to explain and interpret the experimental results. The model presented here allows the pore radius involved in each equilibrium to be determined so that the model exactly reproduces the experimental equilibrium pressure. The close correspondence of pore-volume distributions reconstructed using this model with those based on the nitrogen adsorption/desorption method (Lowell and Shields, 1991) help to validate the model and indicate that hydrate formed in most if not all of the experimental results suggest that porous media have a greater effect on the equilibrium pressure for hydrates that form at lower pressures.

Acknowledgments

This work was completed while J. W. Wilder was a Senior Research Associate of the National Research Council, and was funded by the Office of Fossil Energy, U.S. Department of Energy.

Literature Cited

Cheney, W., and D. Kincaid, *Numerical Mathematics and Computing*, 3rd ed., Brooks/Cole, Pacific Grove, CA, p. 82 (1994)

Clarke, M. A., M. Pooladi-Darvish, and P. R. Bishnoi, "A Method to Predict Equilibrium Conditions of Gas Hydrate Formation in Porous Media," *Ind. Eng. Chem. Res.*, **38**, 2485 (1999).

Clennell, M. B., M. Hovland, J. S. Booth, P. Henry, and W. J. Winters, "Formation of Natural Gas Hydrates in Marine Sediments 1. Conceptual Model of Gas Hydrate Growth Conditioned by Host Sediments Properties," *J. Geophys. Res.*, **104**, 22985 (1999).

de Boer, J. H., *The Structure and Properties of Porous Materials*, Vol. 10, D. H. Everett and F. S. Stone, eds., Buttersworth, London, p. 68 (1958).

Handa, Y. P., and D. Stupin, "Thermodynamic Properties and Dissociation Characteristics of Methane and Propane Hydrates in 70-A-Radius Silica Gel Pores," *J. Phys. Chem.*, **96**, 8599 (1992).

Handa, Y. P., M. Zakrzewski, and C. Fairbridge, "Effect of Restricted Geometries on the Structure and Thermodynamic Properties of Ice," *J. Phys. Chem.*, **96**, 8594 (1992).

Henry, P., M. Thomas, and M. B. Clennell, "Formation of Natural Gas Hydrates in Marine Sediments 2. Thermodynamic Calculations of Stability Conditions in Porous Sediments," *J. Geophys. Res.*, **104**, 23005 (1999).

Holder, G. D., S. P. Zetts, and N. Prodhan, "Phase Behavior in Systems Containing Clathrate Hydrates," *Rev. Chem. Eng.*, **5**, 1 (1988).

Kamath, V. A., "Study of Heat Transfer Characteristics During Dissociation of Gas Hydrates in Porous Media," PhD Diss., Univ. of Pittsburgh, Pittsburgh, PA (1984).

Klauda, J. B., and S. I. Sandler, *Ind. Eng. Chem. Res.*, (2001). (Currently available as an ASAP document on the ACS Web site.)

Lowell, S., and J. E. Shields, *Powder Surface Area and Porosity*, Chapman & Hall, New York, p. 52 (1991).

Makogon, Y. F., *Hydrates of Natural Gas*, PennWell, Tulsa, AZ (1981).

Munck, J., S. Skjoid-Jorgensen, and P. Rasmussen, "Computations of the Formation of Gas Hydrates," *Chem. Eng. Sci.*, **43**, 2661 (1988).

Seshadri, K., J. W. Wilder, and D. H. Smith, "Measurements of Equilibrium Pressures and Temperatures for Propane Hydrate in Silica Gels with Different Pore-Size Distributions," *J. Phys. Chem.*, **105**(13), 2627 (2001).

Sloan, E. D., *Clathrate Hydrates of Natural Gases*, 2nd ed., Dekker, New York (1997).

Uchida, T., T. Ebinuma, and T. Ishizaki, "Dissociation Condition Measurements of Methane Hydrate in Confined Small Porous Glass," *Phys. Chem.*, **103**, 3659 (1999).

van der Waals, J. H., and J. C. Platteeuw, "Clathrate Solutions," *Adv. Chem. Phys.*, **2**, 1 (1959).

Manuscript received Mar. 22, 2001 and revision received July 30, 2001.